A granular Büttiker-Landauer motor
Supplemental information

O. Devauchelle
Université de Paris, Institut de Physique du Globe de Paris,
1 rue Jussieu, CNRS, 75238 Paris, France

P. Popović
Faculty of Physics, University of Belgrade, POB 44, 11001 Belgrade, Serbia

P. Szymczak
Institute of Theoretical Physics, Faculty of Physics,
University of Warsaw, Pasteura 5, 02-093 Warsaw, Poland

A. Abramian
Sorbonne Université, CNRS, Institut Jean Le Rond d'Alembert, F-75005 Paris, France

A. Lazarus
Sorbonne Université, CNRS, Institut Jean Le Rond d'Alembert, F-75005 Paris, France and
Massachusetts Institute of Technology,
Department of Mathematics, Cambridge, MA 02139, USA
(Dated: May 7, 2026)

References to equations, figures, and sections appearing in the present document start with "SM". Otherwise, references point to the main document.

SM1. RANDOM WALK SIMULATION

We consider a random walker in one dimension, the step size ℓ of which depends explicitely on its position x: The length of a step is set by the position of the walker at the onset of the step. For illustration, we make the step size vary according to

$$\ell = \epsilon \left(1 + \gamma x^2\right) , \tag{SM1}$$

where ϵ is the smallest step size, and γ controls the amplitude of the diffusivity gradient. The numerical implementation of this problem is presented in table SM1. After sufficiently many steps, the distribution of the walker's position converges towards a humped histogram (figure SM1). This distribution accords with intuition: the walker is found more often near $x = 0$, where its steps are shorter.

As the time step is set to 1 in this simulation, the diffusivity of the walker scales like $D \sim \ell^2$ and, according to equations (2) and (SM1), its probability density should be proportional to

$$\rho \propto \frac{1}{\left(1 + \gamma x^2\right)^2} , \tag{SM2}$$

an expression to be normalized through a prefactor (ϵ only affects the time required to reach steady state). This prediction matches well the numerical histogram of our toy simulation

```python
from pylab import rand, hist, sign
x = [ 0 ]
for dw in 2*rand(100000) - 1 :
    new_x = x[-1] + 0.05*dw*( 1 + 5*x[-1]**2 )
    if abs( new_x ) > .5 : # boundary condition
        new_x = sign(new_x) - new_x
    x += [ new_x ]
hist( x, bins = 25)
```

TABLE SM1. Python implementation of a one-dimensional random walker with varying diffusivity. The walker is confined on the segment $[-0.5, 0.5]$ by reflecting walls. The step size follows equation (SM1) with $\epsilon = 0.05$ and $\gamma = 5$.

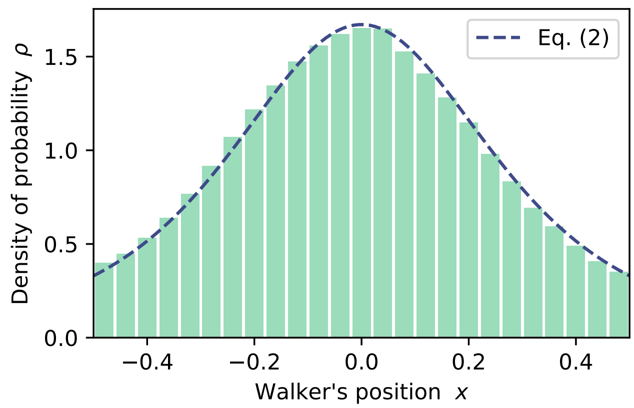

FIG. SM1. Steady-state distribution of a random walker with varying diffusivity. Histogram: random numerical simulation (table SM1). Dashed line: equation (SM2), corresponding to equation (2) with $\epsilon = 0.05$ and $\gamma = 5$, and normalized.

(figure SM1). This good agreement is not necessarily surprising, but the ease with witch it is reached might be. The numerical simulation of Brownian motion, indeed, is a notoriously challenging exercise in computational mathematics, in part because the dynamics should relax towards the Boltzmann equilibrium. For this to happen, one needs to carefully account for hydrodynamic interaction, which changes the diffusivity of a colloidal particle as it approaches a wall (or another particle) [1, 2]. No such refinement is required here, because (ideal) bouncing grains are free from the thermal bath during their jumps—their discrete motion is fully explicit.

SM2. EXPERIMENTS

A. Setup

The corral that contains the grains in the experiments, and the loudspeaker that vibrates it, are mounted on a reclining aluminum frame, which also holds two led panels, the camera and the inclinometer (figure SM2a).

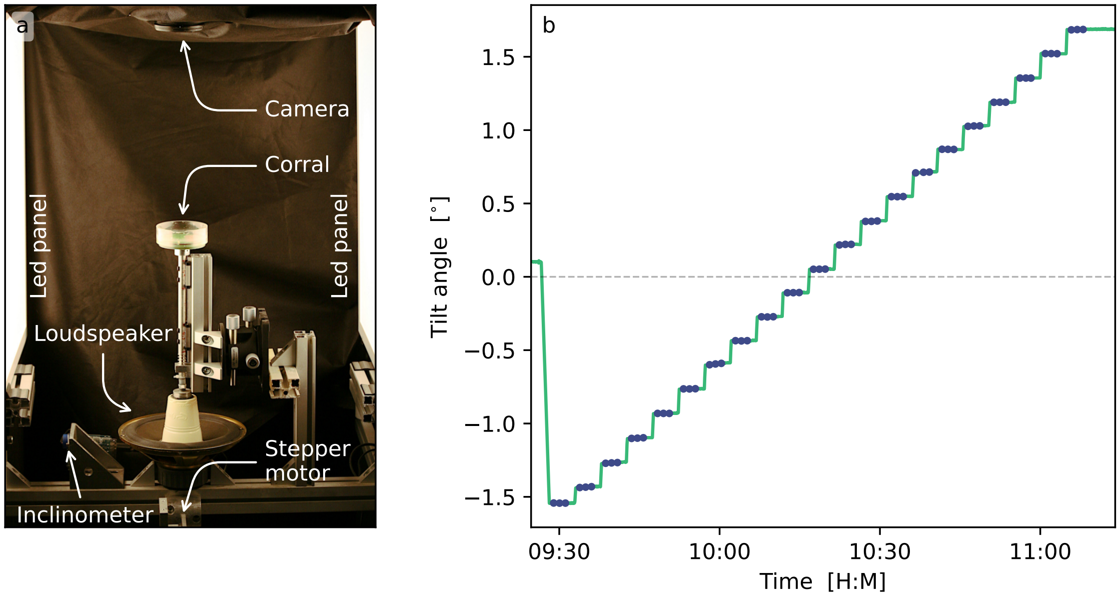

FIG. SM2. a: Experimental setup. The height of the two led panels is 60 cm. The frame that holds the camera and the loudspeaker rotates around the axis that joins the centers of the led panels. This tilt is controlled by the stepper motor. b: Time series of the tilt angle for run C, as measured with the inclinometer. Each dot indicates a 1 min-long movie.

The 8 Ω loudspeaker is driven by a function generator (Hameg HM8030-6) through an analog amplifier (Kemo M034N). We use a sinusoidal signal of frequency 30 or 40 Hz; lower frequencies induce higher bounces, whereas higher frequencies can resonate with the structure.

A stepper motor (Zaber NM23A200) drives a micrometric translating optical stage, which pushes the reclining frame in the y direction (figure 1a), thus introducing a small component of gravity along the y axis without perturbing the lighting nor the position of the camera relative to the corral. We control the stepper motor with an Arduino Motor Shield. Each step of the motor induces 0.0021° of tilt. The tilt of the frame is recorded by the capacitive inclinometer (Meiri ME 26410), the analog output of which is amplified through an analog-to-digital converter (Microchip MCP3424), and recorded by an Arduino board. Overall, we can measure the tilt angle with a precision better than 0.01°.

A 3-axis optical stage holds the vertical rail along which the shaft translates to transmit the vibration from the loudspeaker to the corral. This stage allows us to finely adjust the horizontalness of the corral. The membrane of the loudspeaker accommodates the deformation this adjustment induces.

The camera (Canon EOS 600D) is controlled via its USB port with the Linux library `gPhoto2` [3]. The 50 FPS, one-minute long movies it records are downloaded to the controlling computer before each change of the tilt angle.

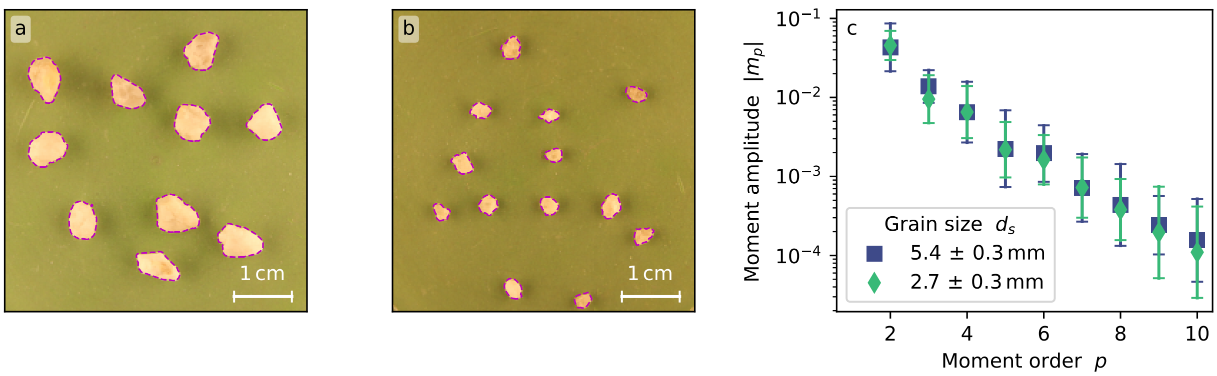

FIG. SM3. a,b: Quartz grains used in the experiments. Dashed magenta lines show edge detection. c: Two-dimensional moments of the grains shown in a,b. Error bars show logarithmic standard deviations over each set of grains. Grain size d_s is the average square root of the grains' area.

B. Grains

The particles used in the experiment are angular quartz grains (figure SM3a,b). The irregularity of their shape contributes to the randomness of their bounces; to characterize it, we take two pictures of about 10 grains at high resolution ($32\,\mathrm{px\,mm^{-1}}$), and detect their edge based on the saturation of their color (figure SM3a,b). To the eye, the grains' shape seems independent of their size. To quantify this observation, we define the two-dimensional, order-p moment of a closed contour $\mathcal{C}$ as

$$\mathcal{M}_p = \iint_{\mathcal{C}} z^p \,\mathrm{d}x\,\mathrm{d}y \tag{SM3}$$

where $z = x + iy$ is the complex coordinate in the plane. Complex notation makes this expression handy, and elementary complex analysis allows one to turn the above expression into a contour integral along $\mathcal{C}$, which is numerically convenient. The order p of the moment can be interpreted as the wavenumber of a Fourier transform along the contour.

Clearly, $\mathcal{M}_0$ is the area of a grain's image, and $\mathcal{M}_1/\mathcal{M}_0$ the complex coordinate of its (two-dimensional) center of mass. We are now ready to define a dimensionless coordinate as

$$\tilde{z} = \tilde{x} + i\tilde{y} = \frac{z - \mathcal{M}_1/\mathcal{M}_0}{\sqrt{\mathcal{M}_0}} \tag{SM4}$$

and use it to compute the dimensionless moments of the grains:

$$m_p = \iint_{\mathcal{C}} \tilde{z}^p \,\mathrm{d}\tilde{x}\,\mathrm{d}\tilde{y}\,. \tag{SM5}$$

By definition, $m_0 = 1$ and $m_1 = 0$. Some of the next moments are represented in figure SM3c for two grain sizes. The spectra are hardly distinguishable, supporting our first impression that the grains' shape is independent of size. One can note, however, that the value of m_3 is somewhat lower for smaller grains, suggesting that bigger grains might be slightly rougher than smaller ones.

Run	A	B	C	D	E	F	G	H
Frequency ν [Hz]	30.6	30.4	29.8	29.8	40.6	40.6	30.4	29.8
Grain size d_s [mm]	5.2 ±0.2	3.2 ±0.8	4.5 ±0.5	2.2 ±0.2	4.2 ±0.2	3.5 ±0.5	2.2 ±0.2	2.2 ±0.2
Tilt steps	20	10	20	10	10	10	10	10
Tilt range [°]	[-1.6, 1.6]	[-0.9, 1.3]	[-1.5, 1.7]	[-1.0, 1.1]	[-2.1, 1.2]	[-1.5, 1.8]	[-1.0, 1.2]	[-0.9, 1.2]
Movies per step	3	3	3	3	2	3	3	3
Diffusivity								
D_{hard} [$\text{cm}^2\,\text{s}^{-1}$]	2.3 ±0.7	2.9 ±0.5	1.8 ±0.8	1.8 ±0.6	0.9 ±0.4	1.4 ±0.3	2.3 ±0.3	2.8 ±0.7
D_{soft} [$\text{cm}^2\,\text{s}^{-1}$]	4.4 ±3.2	3.9 ±3.1	5.4 ±3.7	3.5 ±2.2	3.3 ±1.7	3.8 ±2.1	3.0 ±2.0	4.6 ±2.9
Velocity (RMS)								
v_{hard} [$\text{cm}\,\text{s}^{-1}$]	10.5 ±3.1	10.7 ±2.0	9.0 ±4.6	9.2 ±3.3	6.8 ±2.4	8.4 ±3.6	9.9 ±1.6	11.3 ±3.5
v_{soft} [$\text{cm}\,\text{s}^{-1}$]	14.6 ±3.2	12.8 ±3.0	14.5 ±4.0	12.2 ±1.9	11.7 ±3.4	11.9 ±3.4	11.4 ±2.6	13.9 ±2.6
Surface density								
$10^3\,\rho_{\text{hard}}$ [cm^{-2}]	26 ±0.3	25 ±0.3	28 ±0.4	27 ±0.2	28 ±0.5	28 ±0.5	25 ±0.3	26 ±0.3
$10^3\,\rho_{\text{soft}}$ [cm^{-2}]	13 ±0.9	16 ±1.1	10 ±1.4	13 ±0.7	8 ±1.6	9 ±1.4	18 ±1.0	15 ±0.8
Collision prob.								
$N\rho\ell d_s$ [%]	7	5	5	2	3	3	3	4

TABLE SM2. Experimental parameters. Numbers in gray indicate sieves size for d_s, difference between autocorrelation and dispersion for D, and standard deviation computed over a series of movies, for v and ρ. Surface densities are measured on a horizontal corral. Collision probability estimated with the highest density ρ_{hard}, a total number of grains $N = 5$, and equation (SM6).

C. Procedure

An experiment begins with the reclining frame held in vertical position. We first place a uniform corral (without any soft pad) atop the shaft, and populate it with a small number of grains (about 5). We then select a vibrating frequency (table SM2) and adjust the amplitude of the vibration manually, until the grains remain detached from the surface of the corral (we do not measure the vibration amplitude; it is less than a mm). At the frequencies we use, there is not much margin of adjustment for the amplitude—grains do not jump at low amplitude, and can jump over the rim of the corral at high amplitude. Once set, the vibration parameters will not change during an experiment.

The next step is to manually adjust the tilt of the corral with the 3-axis stage. The corral is close to horizontal when the grains roam across it uniformly, which we evaluate with the naked eye. (This method proved more reliable than using a digital angle gauge.) The zero of the tilt will be pinpointed later, based on the grains' trajectories (section SM2 D). At this stage, we swap the uniform corral for one with a soft pad, and the experiment starts.

An experimental run consists in varying the tilt of the setup with the stepper motor, and recording three one-minute movies for each value of the tilt (figure SM2b). Before shooting the first movie of each series, we wait at least one minute to let the grains reach steady state. We use 10 or 20 tilt steps, over a range of a few degrees (table SM2). A complete

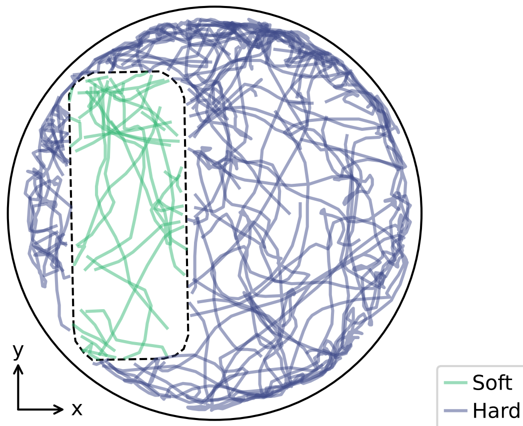

FIG. SM4. Trajectories in a horizontal corral (run C). Less than 20 % of the trajectories associated with a single movie are represented.

series of measurement lasts about an hour and a half. At the end of each run, we remove the grains from the corral, and take a short movie of the empty corral, which we will use as a background for grain tracking.

D. Grain tracking

Each experimental run yields about 60 one-minute long movies, that is, about 10^5 images of size 1280×720 px. This corresponds to a spatial resolution of 0.14 mm px^{-1}. The quartz grains appear as cream-colored, irregular spots about 30 pixels in size (figure 1b). Having no well-defined hue, they are easily distinguished from the green or pink background based on their saturation. To locate the grains, we smooth the saturation of each image with a Gaussian filter of size comparable to the grains' (typically 10 px, depending on grain size), and find the local maxima with the `peak_local_max` function of the `scikit-image` Python library [4].

To reconstruct trajectories, we need to match the peaks associated with each grain in two successive images. This is done through global minimization of distances, with the Munkres algorithm (figure SM4) [5]. Some trajectories are broken, for instance when two grains come two close to each other or, more rarely, when a grain orients itself with respect to the lighting as to appear too dark for detection. On average, over a total of more than 10^5 trajectories, we can track a grain over 45 successive images, that is, over about one second. We could improve the quality of the tracking by reducing the number of grains used in each experiment, but we would then need proportionally longer experiments.

To test how independent the grains are from each other, we can estimate the probability of a collision during a jump, namely $N\rho\ell d_s$, where ℓ is the step size. Based on the ballistic approximation,

$$\ell = \frac{2v^2 \tan\theta}{g} \,. \tag{SM6}$$

The corresponding probability is always less than 10 % in our experiments, when the corral is horizontal (table SM2). When the corral is strongly tilted, however, the gathering of

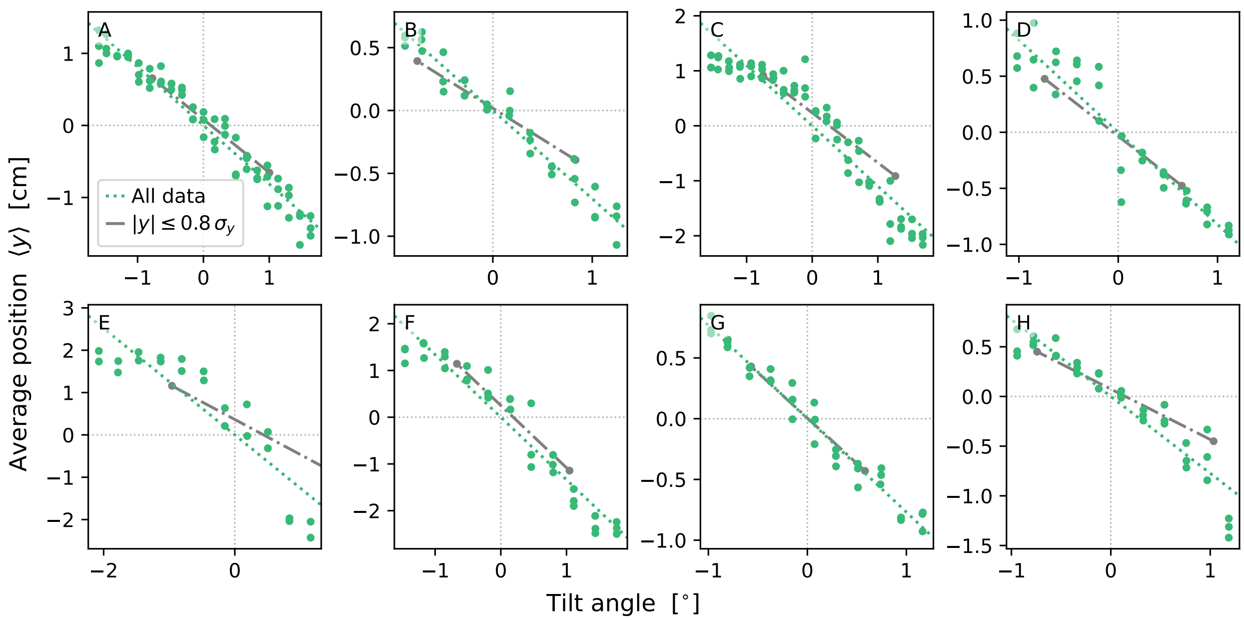

FIG. SM5. Average position of the grains, $\langle y \rangle$, as a function of the tilt angle. Dotted green line: linear fit based on which the zero of the tilt is set (all data included). Dotted-dashed gray line: linear fit restricted to $|y| < 0.8\,\sigma_y$, where σ_y is the standard deviation of y. Label indicates run number (table SM2). The standard deviation of the difference in angle origin based on the two fits is $0.15°$.

the grains near the lower part of the wall makes them likely to interact, but the angular momentum is already very weak when this happens.

We collect the trajectories associated with a movie into a bunch object, as defined by the `BrownTrack` library [6], which we store as a `json` dictionary that can be later opened for analysis. In total, the tracking takes about half an hour of desktop-computer time for each experimental run.

Once the trajectories are collected, we need to find the origin of the tilt angle. To do so, we assume, based on the corral's symmetry with respect to the x-axis, that the average position of the grains along the other axis, $\langle y \rangle$, vanishes when the corral is horizontal (figure SM5). Fitting $\langle y \rangle$ as an affine function of the measured, uncalibrated tilt angle, we find the origin of the tilt. Repeating this procedure for a restricted set of data ($|y| < 0.8\,\sigma_y$, where σ_y is the standard deviation of y), we find that the standard deviation of the origin based on the two fits is $0.15°$—comparable to the dispersion of our measurements.

SM3. FINITE-ELEMENT SIMULATION

We use the finite-element method to solve equation (7), which derives from the Smoluchowski equation when the temperature varies weakly over the corral ($\Delta\beta/\beta_{\mathrm{hard}} \ll 1$). To do so, we use the Python library `pyFreeFem` [7], which wraps the finite-element software `FreeFem++` [8], as shown in figure SM6. This will allow us to compute the density contours and flow lines in figure 3b, and the theoretical curve in figure 3c.

We first express the external potential as $V = fy$, and make all lengths dimensionless by normalizing them with the radius R of the corral. In the weak formulation suited to the

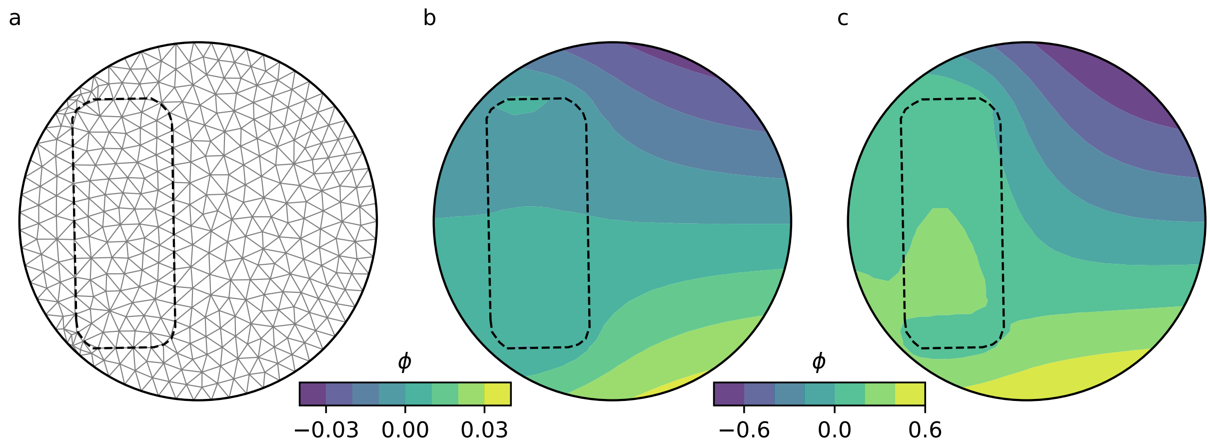

FIG. SM6. Finite-element solution of equation (7). All quantities are dimensionless, as in equation (SM7). a: Triangular mesh on which the finite-element space is defined. b,c: Contours of ϕ for uniform diffusivity ($\gamma = 0.1$ and $\gamma = 3$, respectively). Figure 3 shows the solution for $\gamma = 0.5$.

finite-element method, equation (7) reads

$$\iint_{\text{corral}} e^{-\gamma y} \nabla\psi \cdot \nabla\phi \, \mathrm{d}x \, \mathrm{d}y \; + \; \gamma \iint_{\text{corral}} e^{-\gamma y} H \, \frac{\partial \psi}{\partial y} \, \mathrm{d}x \, \mathrm{d}y = 0 \tag{SM7}$$

where ψ is any test function belonging to the resolution space, $\gamma = \beta_0 f R$ is the only dimensionless parameter of the problem, and spatial dimensions are made dimensionless with R. Since no grain can enter or leave the corral, the boundary contribution is implicit in the weak formulation of the problem.

By itself, equation (SM7) is degenerate, as any constant can be added to its solution ϕ. The missing constraint is mass balance, which requires that the integral of ρ be one. At first order, it reads

$$\iint_{\text{corral}} \frac{\phi}{D} = 0 \, . \tag{SM8}$$

Only at this stage does the distribution of diffusivity affect the solution, in the form of an additive constant. The particle flux $\mathbf{j}$ is independent of this constant, and depends on diffusivity only through multiplication by the constant $\langle 1/D \rangle_B$ in equation (8). In figures SM6 and 3b, for simplicity, we assume that diffusivity is uniform to represent ϕ or ρ/ρ_0. Any other choice would affect the values of the contour lines, but not their shape.

SM4. ANGULAR MOMENTUM

We estimate the average angular momentum of the grains, M, based on our experimental trajectories:

$$M \approx \left\langle \frac{1}{T} \sum_{n=0}^{N-1} \mathbf{x}_n \times \mathbf{x}_{n+1} \right\rangle_{\text{traj.}} , \tag{SM9}$$

where the brackets $\langle \cdot \rangle_{\text{traj.}}$ denote the average over the available trajectories, N is the number of points of a trajectory, $\mathbf{x}_n$ is the recorded position of the grain at index n in that trajectory,

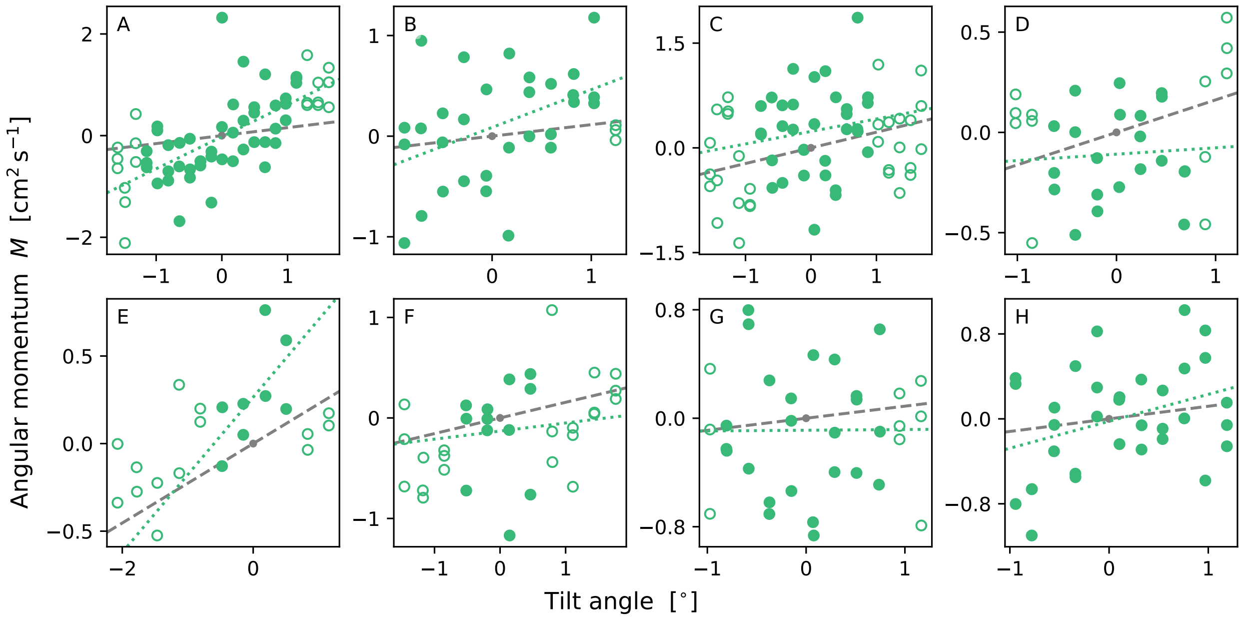

FIG. SM7. Angular momentum as a function of tilt angle. Labels correspond to experimental runs (table SM2). Each data point corresponds to a single experimental movie. Filled dots correspond to expected linear range ($\gamma < 1$). Circles are discarded for fitting. Dotted line: Fitted affine relation. Dashed line: Equation (SM10).

and T is the duration of each trajectory. We can then plot the momentum as a function of the tilt θ of the corral for each experimental movie (figure SM7). Despite the scatter associated to a random walk, the two quantities seem correlated—the Spearman rank coefficient is 0.35 ± 0.1 (standard error) over all runs.

To compare these observations with theory, we first linearize equations (7) and (8) when the variation of the external potential is much smaller than the temperature, that is, $\gamma = \beta_0 f R \ll 1$. (Filled dots in figure SM7 correspond to the weaker constraint $\gamma < 1$.) We then find

$$M \approx -\frac{a_{\text{soft}}}{\pi R^2} \Delta\beta \, \langle D \rangle_h \, x_s \, m \, g \, \theta \tag{SM10}$$

where $\langle\cdot\rangle_h$ is the harmonic average, a_{soft} and x_s are the area and the position of the center of mass of the soft pad, and θ is the tilt angle (thus $f = m\,g\,\theta$). We evaluate the inverse temperature βm based on the grains' trajectories over the hard disk and the soft pad, which allows us to represent equation (SM10) in figure SM7. On average, the ratio between the slope of a fitted affine relation (dotted line) over the theoretical slope (dashed line) is 1.6 ± 0.5 (standard error). The theory is thus compatible with our observations, but the scatter is too large for a definitive answer at this stage. The non-linear relationship presented in figure 3, which allows us to include all our experiments, is more conclusive.

[1] D. L. Ermak and J. A. McCammon, Brownian dynamics with hydrodynamic interactions, The Journal of Chemical Physics **69**, 1352 (1978).

[2] A. J. Ladd, Short-time motion of colloidal particles: Numerical simulation via a fluctuating lattice-Boltzmann equation, Physical Review Letters **70**, 1339 (1993).
[3] gPhoto^2 digital-camera Unix software, `http://gphoto.org/`.
[4] S. van der Walt, J. L. Schönberger, J. Nunez-Iglesias, F. Boulogne, J. D. Warner, N. Yager, E. Gouillart, T. Yu, and the scikit-image contributors, scikit-image: image processing in Python, PeerJ **2**, e453 (2014), `https://scikit-image.org/`.
[5] Munkres (Hungarian) algorithm for the assignment problem in Python, `https://pypi.org/project/munkres/`.
[6] BrownTrack Python library, `https://github.com/odevauchelle/BrownTrack/tree/main`.
[7] pyFreeFem Python library, `https://github.com/odevauchelle/pyFreeFem`.
[8] F. Hecht, New development in FreeFem++, J. Numer. Math. **20**, 251 (2012).